Author(s): Wu, F. & Queipo, P. & Nasibulin, A. & Tsuneta, T. & Wang, T. H. & Kauppinen, E. & Hakonen, Pertti J.

Title: Shot Noise with Interaction Effects in Single-Walled Carbon Nanotubes

Year: 2007

Version: Final published version

Please cite the original version:

Wu, F. & Queipo, P. & Nasibulin, A. & Tsuneta, T. & Wang, T. H. & Kauppinen, E. & Hakonen, Pertti J. 2007. Shot Noise with Interaction Effects in Single-Walled Carbon Nanotubes. Physical Review Letters. Volume 99, Issue 15. 156803/1-4. ISSN 0031-9007 (printed). DOI: 10.1103/physrevlett.99.156803

Shot Noise with Interaction Effects in Single-Walled Carbon Nanotubes

F. Wu,[1] P. Queipo,[2] A. Nasibulin,[2] T. Tsuneta,[1] T. H. Wang,[3] E. Kauppinen,[2] and P. J. Hakonen[1]

[1]*Low Temperature Laboratory, Helsinki University of Technology, P.O. Box 2200, 02015 HUT, Espoo, Finland*
[2]*Center for New Materials, Helsinki University of Technology, P.O. Box 1100, 02015 HUT, Espoo, Finland*
[3]*Institute of Physics, Chinese Academy of Sciences, 100080, Beijing, China*

(Received 19 February 2007; revised manuscript received 1 June 2007; published 11 October 2007)

We have measured shot noise in single-walled carbon nanotubes with good contacts at 4.2 K at low frequencies ($f = 600$–850 MHz). We find a strong modulation of shot noise over the Fabry-Perot pattern; in terms of the differential Fano factor the variation ranges over 0.4–1.2. The shot noise variation, in combination with differential conductance, is analyzed using two (spin-degenerate) modes with different, energy-dependent transmission coefficients. Deviations from the predictions from Landauer-Buttiker formalism are assigned to electron-electron interactions.

DOI: 10.1103/PhysRevLett.99.156803 PACS numbers: 73.63.Fg, 73.50.Td

Shot noise measurements have proven to be useful in providing information on the fundamental conduction mechanisms in mesoscopic conductors [1]. For example, shot noise has been utilized to determine the effective charge of quasiparticles in fractional quantum Hall systems [2,3]. In multiterminal conductors, current-current cross-correlations have been employed for investigating the fermionic nature of charge carriers [4,5]. Also in single-walled carbon nanotubes (SWNT), noise is expected to be a valuable tool for studying the physics of charged elementary excitations [6–13].

Liang *et al.* in Ref. [14] have shown that SWNTs may act as waveguides for electronic transport. They employed a scattering matrix approach to show that the results could be understood in terms of Fabry-Perot (FP) type of interference in which reflection at the contacts played a crucial role [14,15]. Shot noise in the FP regime was recently studied at 4.2 K by Kim *et al.* [12] who found power law dependence at low bias voltages as well as oscillations at larger bias. These findings were assigned to Luttinger-liquid behavior of SWNTs.

We have measured shot noise and ac conductance in a SWNT sample which displays a rather asymmetric Fabry-Perot resonance pattern. The interference pattern has a strong modulation, mostly dominated by a single mode: the contribution from the second is only about $0.1 \times 2e^2/h$. We find a strong modulation of noise over the FP pattern which we characterize in terms of a differential Fano-factor F_d. The resonance condition is reflected as a strong suppression of shot noise with $F_d \simeq 0.4$ while the destructive interference yields $F_d \simeq 1.2$. We find the variation of Fano-factor stronger than expected for a regular quantum conductor model with energy-dependent transmission coefficients. Our results, reported here up to energies of $\sim$10 meV (2 times the level spacing), do not reflect Luttinger-liquid physics, but they can be understood qualitatively within the framework interacting coherent conductor model [16].

The current in a quantum dot can be expressed in terms of the energy ϵ dependent transmission coefficient $I = \frac{2e}{h}\int_0^{eV}\sum_{i=1}^{N}\tau_i(\epsilon, V)d\epsilon$, where $\tau_i(\epsilon, V)$ denotes the transmission coefficient of spin-degenerate mode i and we assume that the voltage is applied to one terminal only. For differential conductance G_d, this yields

$$G_d = \frac{dI}{dV} = \frac{d}{dV}\left(\frac{2e}{h}\int_0^{eV}\sum_{i=1}^{N}\tau_i(\epsilon, V)d\epsilon\right). \quad (1)$$

In the case of noninteracting electrons, $\tau(\epsilon, V)$ is voltage independent and Eq. (1) reduces to $dI/dV = G_0\sum_{i=1}^{N}\tau_i(eV)$ with $G_0 = 2e^2/h$.

The low-frequency shot noise is given by

$$S(V) = \int dt\langle\delta I(t)\delta I(0) + \delta I(0)\delta I(t)\rangle = \frac{4e^2}{h}\int_0^{eV}\sum_{i=1}^{N}\tau_i(\epsilon)[1-\tau_i(\epsilon)]d\epsilon, \quad (2)$$

where $\delta I(t) = I(t) - \langle I(t)\rangle$ at voltage V, and the current-current correlator reduces to the latter form in the absence of interactions. By combining Eqs. (1) and (2) we may define the differential Fano factor as

$$F_d = \frac{1}{2e}\frac{dS}{dV}\Big/\frac{dI}{dV} = \frac{1}{2e}\frac{dS}{dI}. \quad (3)$$

This is a quantity that we probe in our sensitive noise measurements based on lock-in detection on modulated noise signal.

In the above formulas, it is assumed that $eV \gg k_BT$. In the crossover regime with $eV \sim k_BT$, one may write for the excess noise, the difference of current noise and thermal noise

$$S(I) - S(0) = \frac{4k_BT}{R(0)}\left(KF\frac{eV}{2k_BT}\coth\left(\frac{eV}{2k_BT}\right) - F_0\right), \quad (4)$$

where $S(0)$ specifies the noise at zero bias, $R(0) = V/I$ in the limit $V \to 0$, F denotes the Fano-factor (F_0 at $V = 0$) and $K = R(0)/(V/I)$ accounts for the nonlinearities of the I-V curve. The left side can be identified as $\int_0^I \frac{dS}{dI}dI = \int_0^I 2eF_d dI$. Hence, Eq. (4) provides an interpolation for-

mula for the average Fano factor $\tilde{F} = \frac{1}{I}\int_0^I F_d dI$ that is obtained from our measurements. Note that $\tilde{F} = (S(I) - S(0))/(2eI)$ is the quantity that is often used to determine the Fano factor [17]; at large $V \gg k_B T/e$, $\tilde{F}$ is equivalent to F in Eq. (4).

In the nonlinear regime, noise measurements are sensitive to changes in the sample resistance. For our setup, where a sample having a dynamic resistance of R_d is connected to a preamplifier with impedance $R_L = 50\ \Omega$ (see Fig. 2 inset for the equivalent circuit), we may derive

$$\frac{1}{G_{\rm cal}}\frac{1}{R_L}\frac{\Delta P}{\Delta I} = 2eF_d - 2eF_d\frac{2R_L}{R_d} - 2i_n^2 R_d R_L \frac{\partial^2 I}{\partial V^2}, \quad (5)$$

which relates the measured, gain-adjusted noise power variation $\frac{1}{G_{\rm cal}}\frac{\Delta P}{\Delta I}$ to F_d $(= \frac{1}{2e}\frac{dS}{dV}/\frac{dI}{dV})$. The second term on the right describes the first order correction in measured shot noise due to changes in R_d while the third term takes into account corrections caused by the total system noise due to nonlinearities; i.e., i_n^2 marks the full noise at the operating point, including the preamplifier noise. The calibrated gain $G_{\rm cal}$ remains fixed within the factor $1 + \frac{2R_L}{R_T} - \frac{2R_L}{R_d}$, where R_T denotes the resistance of the tunnel junction employed in the calibration.

In our measurement setup, bias tees are used to separate dc bias and the bias-dependent noise signal at microwave frequencies. We use a liquid-helium-cooled low-noise amplifier (LNA) [18] with operating frequency range of $f =$ 600–950 MHz. The noise signal is band limited to 600–850 MHz in order to avoid pickup from mobile phones working at 940 MHz despite a Faraday cage. After amplification of 80 dB, the signal was detected by a zero-bias Schottky diode with 0.5 mV/μW. For calibration purposes, we use a microwave switch that connects the amplifier chain either to a nanotube sample or to a tunnel junction. For details we refer to Ref. [19].

Noise was measured using three different methods (in the order of increasing sensitivity): (i) noise at dc current, (ii) lock-in detection of noise using sine-wave modulation of current, $I = I_{\rm DC} + \delta I \sin(\omega t)$, where $I_{\rm DC} \gg \delta I$, (iii) current modulation by square-wave $\Pi(t)$, $I = I_{\rm DC} + I_m \Pi(t/t_0)$, where $I_{\rm DC} = I_m/2$. The calibration constants for each scheme were measured making similar experiments on a tunnel junction sample of a resistance of $R_T =$ 22 kΩ. The data reported in this Letter are mostly measured using method (ii). Data obtained using method (iii) agreed well with those measured with method (ii), but the implementation of the nonlinearity corrections turned out to be more problematic for method (iii) than for (ii). In addition to the above measurement schemes, we also performed experiments along method (ii) where the dc bias was kept at zero and the noise modulation was measured at frequency 2ω while having the excitation at ω. By extrapolating the results of this method to $\delta I = 0$, we obtain the "zero-bias" Fano factor. In the corrections using Eq. (5), we have estimated $i_n^2 = 2.5 \times 10^{-24}$ A^2, which is obtained from the noise temperature $T_N = 3.5$ K of our cooled LNA [18] using $i_n^2 = 4k_B T_N/R_L$ for the unmatched case, as $4k_B T_N/R_L$ is much larger than the shot noise generator $S_i = \tilde{F} \cdot 2eI$.

Our nanotube sample was made using surface chemical vapor-deposition (CVD) growth with Fe catalyst. The length was $L = 0.7\ \mu$m and the diameter $\phi = 2$ nm. The contacts on the nanotube were made using standard e-beam overlay lithography. In the contacts, 10 nm of Ti was employed as a sticking layer before depositing 70 nm of Al, followed by 5 nm of Ti. The width of the two contacts was 200 nm and the separation between the them was 0.3 μm. The strongly doped silicon substrate was employed as a back gate, separated from the sample by 100 nm of SiO_2.

A scan of differential conductance $G_d = \frac{dI}{dV}$ is displayed in Fig. 1. Clear maxima or minima in G_d with gate modulation are observed at zero bias, but no characteristic features of odd or even effects that are found in the Kondo regime of carbon nanotubes [20]. Therefore, we conclude that the pattern is due to FP interference even though it appears more asymmetrically-striped than observed typically [13,14]. The maximum G_d is only about $1.0G_0 (= 2e^2/h)$ which indicates a rather weak coupling to one of the orbital modes of our nanotube sample. The contrast of the fringes is clearly stronger than 10%–30% found in Ref. [14]. This may be connected with the fact that in our sample we are dealing mostly with interference within one mode.

To reach the Fabry-Perot regime, the quality of contacts has to be good [14]. This was investigated by making a separate cooldown to 60 mK. No obvious change was observed in the $G_d(V, V_g)$ pattern, indicating that "odd-even" Kondo features do not appear even at dilution refrigerator temperatures. In this 2nd cooldown, strong proximity-induced supercurrent was observed in the nano-

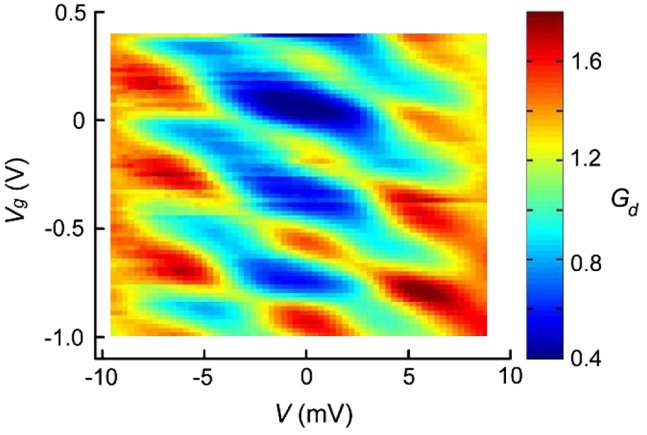

FIG. 1 (color online). Differential conductance G_d on the plane spanned by bias voltage V and gate voltage V_g. The scale bar is given on the right in units of $e^2/h (= G_0/2)$.

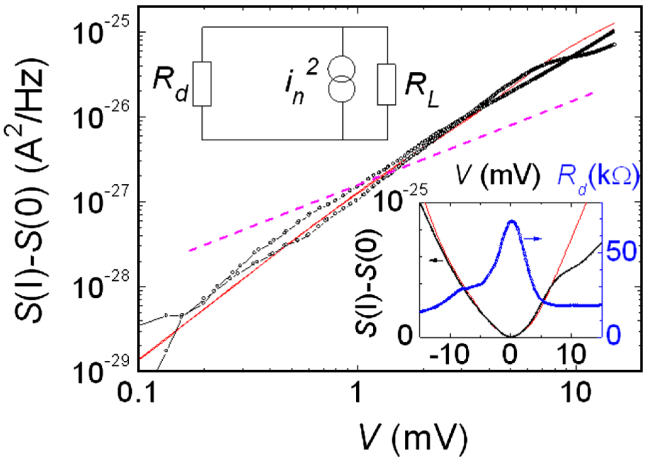

FIG. 2 (color online). Excess noise $S(I) - S(0)$ vs bias voltage $V > 0$ (○) and $V < 0$ (●) at $V_g = 0.04$ V. Red curve illustrates an evaluation of Eq. (4) using $F = 0.65$ and the experimentally determined value $R(0)/(V/I)$. The dashed line refers to exponent $\beta = 1$. The bottom inset displays the data on linear scale (in A^2/Hz). The inset on top displays the electrical equivalent model employed to calculate the coupling of the current fluctuations as well as the corrections due to nonlinearities.

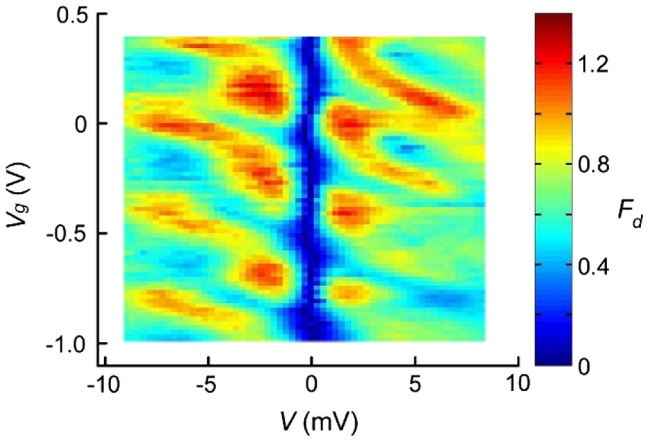

FIG. 3 (color online). Differential Fano factor F_d on V_g vs V plane. The scale bar is given on the right.

tube, which is another indication that the quality of the contacts is sufficient for the FP resonances. Furthermore, in our third cooldown, we were able to observe Kondo-type features. Such a change in the contacts is understandable as cooldowns produce strain that may alter the contact configuration by a tiny amount.

Shot noise data (excess noise $S(I) - S(0)$) using small voltage bias $V = 0.1$–10 mV at $V_g = 0.04$ V are displayed in Fig. 2. The data can be fitted using an apparent power law $[S(I) - S(0)] \propto V^\beta$ with $\beta = 1.7$. This is clearly larger than the exponent $\beta = 0.64$ found in Ref. [12] at $V = 0.1$–10 mV, also at 4.2 K. In Fig. 2, our data are compared with the crossover formula of Eq. (4) using a Fano factor $F = 0.65$, together with the experimentally measured (voltage-dependent) ratio for K. The measured Fano factor is not exactly constant but, nevertheless, there is a good agreement between the measured data and Eq. (4). Thus, in contrast to Ref. [12], we have to conclude that Luttinger-liquid behavior is not necessary to explain the power law dependence in our data.

The measured data [using method (II)] on differential Fano-factor are displayed in Fig. 3. The picture reflects, more or less, the pattern of G_d in Fig. 1: ridges of large (small) F_d follow the ridges of small (large) G_d, similar to behavior in noninteracting, one mode conductor. The swing of F_d, however, exceeds 1, which is the upper limit in Landauer-Buttiker type of formalism for quantum dots and quantum point contacts. At $V_g = 0$, we checked the low bias Fano-factor by measuring noise at 2ω and varied the ac-modulation without any dc component. We obtained $F = 0.6 \pm 0.2$ as the modulation $\delta I \to 0$, which coincides with a smooth continuation of the data in Fig. 3.

In Fig. 4, we interrelate the measured noise and conductance from Figs. 1 and 3 as suggested by Eqs. (1) and (3). At $V = -6.2$ mV in Fig. 4(a), $\tilde{F}$ does not display any oscillations as a function of gate voltage, only gradual large scale variation. The relation between $\tilde{F}$ and $G = I/V$, displayed in Fig. 4(b), appears linear. At other bias values, this dependence is similar to that of the differential quantities displayed in Fig. 4(c). The linear relation between $\tilde{F}$ and $G = I/V$ can be explained using both interacting and noninteracting electron theory [21]. For F_d, however, the noninteracting theory does not work. The dependence of F_d and G_d on V_g is found oscillatory with a small relative phase shift, which leads to ellipses in parametrically plotted curves of $F_d(V_g)$ vs $G_d(V_g)$ in Fig. 4(c). At $V > 0$, the

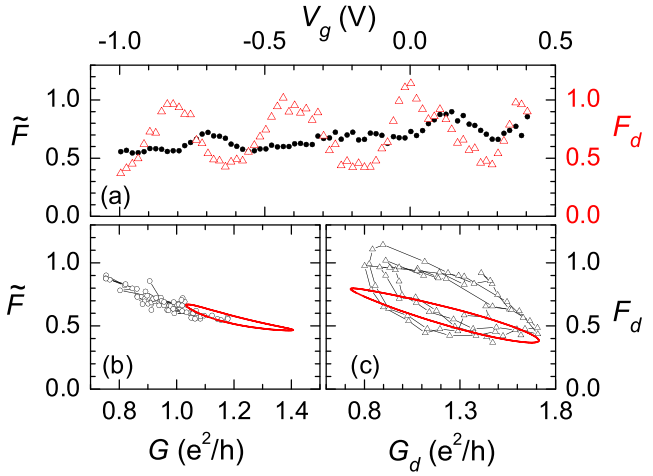

FIG. 4 (color online). Plots obtained using data of Figs. 1 and 3 at $V = -6.2$ mV. (a) Average differential Fano factor $\tilde{F} = \frac{1}{I} \times \int_0^I F_d dI$ (●) and differential Fano factor $F_d = \frac{1}{2e}\frac{dS}{dI}$ (△) as a function of V_g. (b) $\tilde{F}$ vs total conductance $G = I/V$ plotted parametrically by varying V_g. (c) F_d vs G_d plotted parametrically by varying V_g; F_d varies in a clockwise manner with growing V_g. For the overlayed curves, see text.

relations between noise and conductance are similar, including unchanged rotation direction in the parametrically plotted ellipses.

To test in more detail the validity of the Landauer-Buttiker theory, we have made a comparison by assuming two-beam interference so that the transmission coefficients in the FP regime can be parametrized by

$$\tau_i(\epsilon, V_g) = \bar{\tau}_i + m_i \cos[V_g/\Delta V_g \pm \epsilon/(e\Delta V) + \varphi_i], \quad (6)$$

where $i = 1$ or 2 is the number of the mode, $\bar{\tau}_i$ denotes the average value of their transmission, m_i gives the modulation depth of τ_i, and $\varphi_1 - \varphi_2$ specifies the relative phase difference of the transmission modulation. This form yields the interference-induced modulation of transmission coefficients along V_g and V axes with periods ΔV_g and ΔV, respectively. For the FP resonance, one may write $\Delta V_g = \frac{C_\Sigma}{C_g} \frac{\hbar v_F}{e} \Delta k$, which relates the change in the k vectors of the modes to the shift of chemical potential by gate voltage; C_Σ and C_g denote the total and gate capacitances, respectively, and v_F is the Fermi velocity. The curve in Fig. 4 illustrates the result of a calculation for $\tilde{F}$ and F_d using Eqs. (2) and (3) with parameters: $\bar{\tau}_1 = 0.48$, $\bar{\tau}_2 = 0.13$, $\varphi_1 - \varphi_2 = 0$, and $m_i = 0.5\bar{\tau}_i$ [22]. The model accounts for the main features of our data. It reproduces qualitatively deformed ellipses in the parametric plots of $F(V_g)$ and $F_d(V_g)$ vs $G_d(V_g)$, and the elongated shape (even with zero width) tracks, though weakly, the variation found in the experiments. According to this model, the asymmetry of mode conductances is nearly fourfold: $\bar{\tau}_1/\bar{\tau}_2 = 3.7$.

The calculated curve in Fig. 4, however, falls clearly short of the width of the measured, parametrically plotted ellipse. In addition, the average F_d is clearly above the average value from the noninteracting theory. These observations we assign to interaction effects that would lead to explicit bias voltage dependence of the transmission coefficients in Eq. (6). Our observations are consistent with the calculations of Golubev *et al.* [16] who obtain an increase of the Fano factor in an interacting coherent conductor when transmission is large. In addition, the influence of Coulomb correlations on resonant tunneling has been investigated in Refs. [23,24]. It has been shown that positive correlations between tunneling events (bunching of carriers with enhanced F) may be generated if the tunneling events bring the system towards a state with larger conductance, and likewise for negative correlations if G becomes lowered. This noise modulation mechanism would agree with the enhanced width of the parametrically plotted F_d vs G_d ellipse and, if the conduction is due to holes, it would also fit the direction of rotation.

In summary, using conductance and shot noise measurements, we have obtained evidence for quite asymmetric Fabry-Perot resonances in SWNTs. The Fano as well as the differential Fano factor, ranging between 0.4–0.9 and 0.4–1.2, respectively, were found to depend on conductance either in linear or oscillatory fashion. We performed analysis of our results using energy-dependent transmission coefficients, taking carefully in to account the effects due to nonlinear I-V curves. The measured variation in the differential Fano factor is larger than expected from the Landauer-Buttiker formalism, which indicates additional correlations, both positive and negative, due to electron-electron interactions.

We wish to acknowledge fruitful discussions with S. Andresen, M. Buttiker, G. Cuniberti, R. Danneau, C. Glattli, F. Hekking, T. Heikkilä, T. Kontos, L. Lechner, B. Placais, and P. Virtanen. This work was supported by the TULE programme of the Academy of Finland and by the EU Contract No. FP6-IST-021285-2.

[1] Ya. M. Blanter and M. Büttiker, Phys. Rep. **336**, 1 (2000).
[2] L. Saminadayar *et al.*, Phys. Rev. Lett. **79**, 2526 (1997).
[3] R. de-Picciotto *et al.*, Nature (London) **389**, 162 (1997).
[4] M. Henny *et al.*, Science **284**, 296 (1999).
[5] W. D. Oliver *et al.*, Science **284**, 299 (1999).
[6] C. L. Kane and M. P. A. Fisher, Phys. Rev. Lett. **72**, 724 (1994).
[7] P. E. Roche *et al.*, Eur. Phys. J. B **28**, 217 (2002).
[8] K. V. Pham *et al.*, Phys. Rev. B **68**, 205110 (2003).
[9] B. Trauzettel *et al.*, Phys. Rev. Lett. **92**, 226405 (2004).
[10] E. Onac *et al.*, Phys. Rev. Lett. **96**, 026803 (2006).
[11] P. Recher, N. Y. Kim, and Y. Yamamoto, Phys. Rev. B **74**, 235438 (2006).
[12] N. Y. Kim *et al.*, Phys. Rev. Lett. **99**, 036802 (2007).
[13] T. Kontos *et al.*, arXiv:cond-mat/0703123 have independently realized a similar shot noise experiment as we in the present work.
[14] W. Liang *et al.*, Nature (London) **411**, 665 (2001).
[15] C. S. Peça *et al.*, Phys. Rev. B **68**, 205423 (2003).
[16] D. Golubev *et al.*, Phys. Rev. B **72**, 205417 (2005); A. V. Galaktionov *et al.*, Phys. Rev. B **68**, 085317 (2003).
[17] H. Birk *et al.*, Phys. Rev. Lett. **75**, 1610 (1995).
[18] L. Roschier and P. Hakonen, Cryogenics **44**, 783 (2004).
[19] F. Wu *et al.*, AIP Conf. Proc., **850**, 1482 (2006)
[20] See, J. Nygård, D. H. Cobden, and P. E. Lindelof, Nature (London) **408**, 342 (2000), and references therein.
[21] For example, the noninteracting transport can be modeled as a sum of two modes with a changing transmission coefficient $\tau_1 = (G - \tau_2 * G_0)/(G_0)$ and a small constant one $\tau_2 = 0.2$. The Fano-factor $F(G)$ is lifted above the single mode curve $F = 1 - G/G_0$ due to the small contribution of the second mode $\tau_2 \sim 0.2$.
[22] The symmetry properties of $G(V, V_g)$ fix $\varphi_1 - \varphi_2 \sim 0$, the average G_d sets the sum $\bar{\tau}_1 + \bar{\tau}_2$, while the modulation of $G(V, V_g)$ ridges determines $\bar{\tau}_1/\bar{\tau}_2$. The modulation depth of τ_i was taken the same for both modes, yielding the optimum at 50%.
[23] G. Iannaccone *et al.*, Phys. Rev. Lett. **80**, 1054 (1998).
[24] Ya. M. Blanter and M. Buttiker, Phys. Rev. B **59**, 10 217 (1999).